# Optimum Input and Output Filters for a Single-Phase Rectifier Power Supply

SHASHI B. DEWAN, SENIOR MEMBER, IEEE

*Abstract*—**The "optimum" output filter inductance $L_f$ and the input filter capacitor $C_i$ for a single-phase uncontrolled bridge rectifier employed for low power dc-to-dc converters or inverters is established. The filter $C_i$ is optimized to obtain maximum input power factor, minimum filter inductance, and minimum output dc voltage regulation. A design example is provided and theoretical results have been verified on an experimental model.**

## INTRODUCTION

FOR a power rating up to two kW, the dc input voltage for most dc-to-dc converters and inverters is often provided by means of a single-phase diode bridge rectifier. The output of the rectifier generally consists of a single section $L_f$-$C_f$ filter which provides ripple-free dc voltage and attenuates the harmonics. Assuming the filter capacitance $C_f$ is large in Fig. 1, this paper shows that for a given power output, the inductor $L_f$ size is a compromise between the output dc voltage $V$ variation with load and the input power factor.

A detailed analysis is presented here which provides the relationship between the input power factor and the output dc voltage $V$ when the per unit value of the filter inductor $L_f$ is varied. The theoretical results also show that the best input power factor is achieved if the current $i_0$ is discontinuous under all load conditions and the input filter capacitor $C_i$ is employed. This paper also establishes the optimum operating point for the single-phase bridge rectifier from the view point of maximum input power factor, minimum filter inductance and minimum output voltage $V$ regulation from no-load to full-load. Finally a procedure for the selection of filter ($L_f$, $C_i$) components is illustrated by a design example and the theoretical results have been verified experimentally.

## SIMPLIFYING ASSUMPTIONS

The analysis of the single phase diode bridge rectifier system in Fig. 1 is based upon the following assumptions.

1) The output filter capacitance $C_f$ is assumed to be sufficiently large so that the output voltage $V$ is a ripple-free constant dc voltage.
2) The ac source is considered ideal.
3) The losses in inductor $L_f$ and the bridge rectifier are neglected.

Paper IPCSD 80-1, approved by the Static Power Converter Committee of the Industry Applications Society for presentation at the 1980 Industry Applications Society Annual Meeting, Cincinnati, OH, September 28–October 3. Manuscript released for publication November 11, 1980.

The author is with the Department of Electrical Engineering, the University of Toronto, Toronto, ON, Canada M5S 1A4.

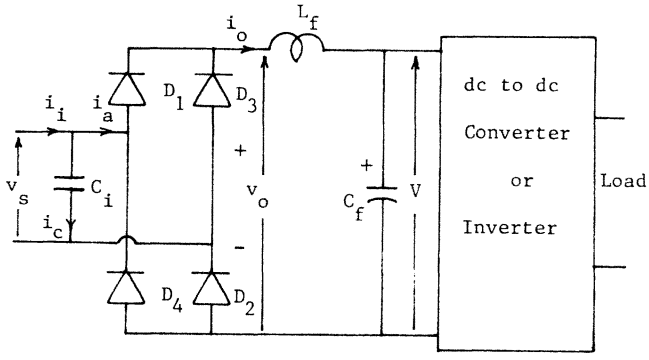


Fig. 1. Single-phase diode bridge rectifier with "optimum" filter.

4) The load is modeled as a variable resistance since the effect of high frequency ripple is negligible as per assumption 1).

*Modes of Operation:* Based upon the instant at which the current $i_0$ goes to zero, the rectifier system in Fig. 1 has three possible modes of operation.

*Discontinuous Mode I* (Fig. 2): The bridge rectifier operates in the discontinuous mode I if the output current $i_0$ is discontinuous and goes to zero before $\omega t = \pi$.

*Discontinuous Mode II* (Fig. 3): The bridge rectifier operates in the discontinuous mode II if the output current $i_0$ is discontinuous and goes to zero at $\pi < \omega t < \pi + \alpha$.

*Continuous Mode* (Fig. 4): The bridge rectifier operates in the continuous mode if the output current $i_0$ never falls to zero.

### *Analysis of the Rectifier in Discontinuous Mode I*

The voltage and current waveforms for discontinuous mode I operation of the rectifier are shown in Fig. 2. The analysis of this mode is presented in the following [1]-[4]:

$$v_s = \sqrt{2}E \sin \omega t \tag{1}$$

$$V_{\text{base}} = \sqrt{2}E$$

$$Z_{\text{base}} = \omega L_f \tag{2}$$

$$I_{\text{base}} = \sqrt{2}E/(\omega L_f)$$

$$m = V/(\sqrt{2}E). \tag{3}$$

The angle $\alpha$ at which diodes $D_1$ and $D_2$ conduction begins ($v_s = V$) is given by

$$\alpha = \sin^{-1} m. \tag{4}$$

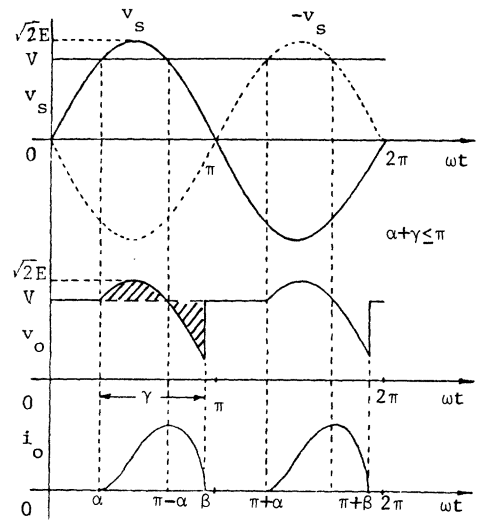


Fig. 2. Time variation of currents and voltages in circuit of Fig. 1 with discontinuous mode I.

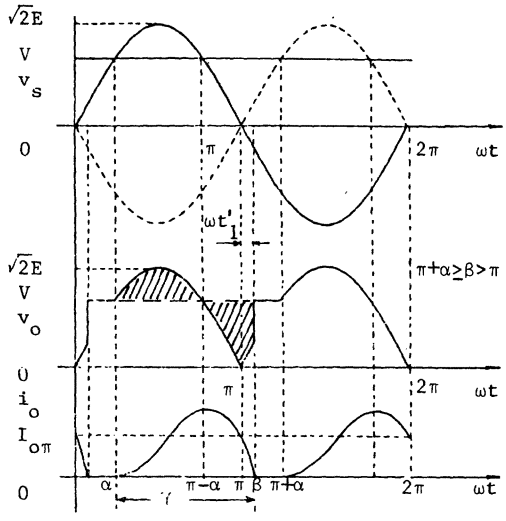


Fig. 3. Time variation of currents and voltages in circuit of Fig. 1 with discontinuous mode II.

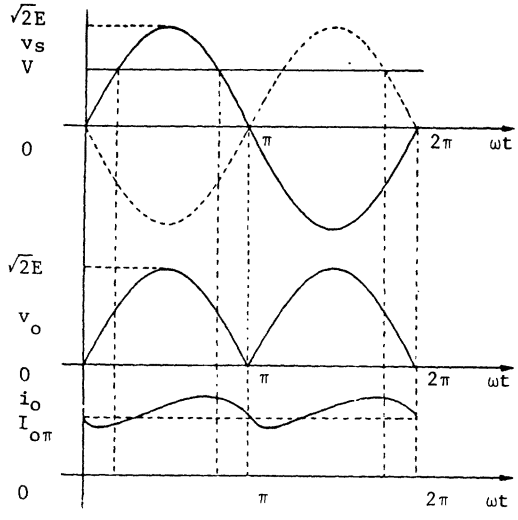


Fig. 4. Time variation of currents and voltages in circuit of Fig. 1 with continuous current mode.

To obtain the conduction angle $\gamma$ notice that the two cross-hatched areas in Fig. 2 have the same volt-seconds, i.e.,

$$\int_{\alpha}^{\pi-\alpha} \sqrt{2}E \sin \omega t d(\omega t) - V(\pi - 2\alpha)$$

$$= V(\beta - \pi + \alpha) - \int_{\pi-\alpha}^{\beta} \sqrt{2}E \sin \omega t \, d(\omega t) \tag{5}$$

where

$$\beta = \gamma + \alpha. \tag{6}$$

From (3), (5), and (6) the following equation results, from which $\gamma$ is calculated.

$$\cos \alpha - \cos(\alpha + \gamma) - m\gamma = 0. \tag{7}$$

The variations of $i_0$ during conduction angle $\gamma$ is obtained from

$$\sqrt{2}E \sin \omega t - V = L_f \cdot di_0/dt, \qquad \alpha \leqslant \omega t \leqslant \pi \tag{8}$$

in which $i_0 = 0$ at $\omega t = \alpha$. Then

$$i_0 = [\sqrt{2}E(\cos \alpha - \cos \omega t) - V(\omega t - \alpha)]/(\omega L_f),$$
$$\alpha \leqslant \omega t \leqslant \pi. \tag{9}$$

From (2), (3), and (9) the normalized output current becomes

$$i_{0n} = i_0/I_{\text{base}} = \cos \alpha - \cos \omega t - m(\omega t - \alpha),$$
$$\alpha \leqslant \omega t \leqslant \pi. \tag{10}$$

The normalized average output current from (10) is

$$I_{0n} = \frac{1}{\pi} \int_{\alpha}^{\alpha+\gamma} i_{0n} \, d(\omega t)$$

$$= \frac{1}{\pi}[\gamma \cos \alpha + \sin \alpha - \sin(\alpha + \gamma) - m\gamma^2/2],$$
$$\alpha \leqslant \omega t \leqslant \pi \tag{11}$$

and the normalized root-mean-square (rms) output current is given by

$$I_{0rn} = \left[\frac{1}{\pi} \int_{\alpha}^{\alpha+\gamma} {i_{0n}}^2 \, d(\omega t)\right]^{1/2}, \qquad \alpha \leqslant \omega t \leqslant \pi. \tag{12}$$

The input power factor (without $C_i$) is calculated from the following expression in which the normalized rms input current $I_{arn}$ is the same as the normalized rms output current $I_{0rn}$

$$(\text{PF}) = V \cdot I_{0n}/(E \cdot I_{arn})$$
$$= V \cdot I_{0n}/(E \cdot I_{0rn})$$
$$= \sqrt{2}mI_{0n}/I_{0rn}. \tag{13}$$

*Analysis of the Rectifier in Discontinuous Mode II*

The voltage and current waveforms for discontinuous mode II are displayed in Fig. 3. Diodes $D_1$ and $D_2$ start to conduct at angle $\alpha$ given by (4). For that part of the output current $i_0$ in Fig. 3 from $\alpha$ to $\pi$, (8)-(11) also hold so that the normalized output current at $\omega t = \pi$ from (10) results in

$$I_{0\pi n} = \cos\alpha + 1 - m(\pi - \alpha). \tag{14}$$

At $\omega t = \pi$, diodes $D_1$ and $D_2$ are commutated, and diodes $D_3$ and $D_4$ go into conduction. The differential equation for the output current $i_0$ from $\omega t = \pi$ to $\omega t = \beta$ is then given by

$$\sqrt{2}E \sin\omega t' = V + L_f \cdot di_0'/dt' \qquad 0 \leqslant \omega t' \leqslant \alpha \tag{15}$$

in which $\omega t' = \omega t - \pi$.

From (3), (15), and the initial condition specified by (14), the normalized output current from $\pi$ to $\beta$ in Fig. 3 yields

$$i_{0n}' = (1 - \cos\omega t' - m\omega t') + I_{0\pi n}. \tag{16}$$

For operation in the discontinuous mode II, the current $i_{0n}'$ falls to zero at an instant $\omega t' = \omega t_1'$ where $0 < \omega t_1' < \alpha$ and is obtained by solving the equation

$$m\omega t_1' + \cos\omega t_1' = 1 + I_{0\pi n}. \tag{17}$$

Therefore, the conduction angle $\gamma$ is given by

$$\gamma = \pi + \omega t_1' - \alpha. \tag{18}$$

In mode II, the normalized, average, and rms output currents, respectively, are given by

$$I_{0n} = \frac{1}{\pi}\left[\int_\alpha^\pi i_{0n}\, d(\omega t) + \int_0^{\omega t_1'} i_{0n}'\, d(\omega t')\right] \tag{19}$$

and

$$I_{0rn} = \left[\frac{1}{\pi}\left\{\int_\alpha^\pi (i_{0n})^2\, d(\omega t) + \int_0^{\omega t_1'} (i_{0n}')^2\, d(\omega t')\right\}\right]^{1/2} \tag{20}$$

in which $i_{0n}$ and $i_{0n}'$ are provided by (10) and (16). Finally, the input power factor (without $C_i$) in this mode is the same as in mode I and given by (13).

*Analysis of the Rectifier in Continuous Mode*

Fig. 4 shows the current and voltage waveforms of the circuit in Fig. 1 in a continuous mode of operation. The average value of the rectifier output voltage $V_0$ is

$$V_0 = \frac{2}{\pi}\sqrt{2}E \tag{21}$$

and since the value of the output voltage $V$ is the same as $V_0$, (3) and (21) yield

$$m = \frac{V}{\sqrt{2}E} = \frac{2}{\pi} = 0.637. \tag{22}$$

Equation (22) shows that in a continuous mode of operation the value of normalized capacitor voltage $m$ remains constant and equal to $2/\pi$. From [4], the Fourier series of the rectified voltage $v_0$ is

$$v_0 = \sqrt{2}E\left[2/\pi - \sum_{n=2,4,6,\cdots}^{\infty} \frac{4}{\pi(n-1)(n+1)} \cos n\omega t\right] \tag{23}$$

from which the output current results in

$$i_0 = I_0 + \sum_{n=2,4,6,\cdots}^{\infty} C_n \cos n\omega t \tag{24}$$

where

$$I_0 = (2\sqrt{2}E/\pi - V)/r, \tag{25}$$

if $L_f$ has a resistance equal to $r$. However, $r$ is negligible so that the average output current $I_0$ is determined by the load. From Fig. 1 and (2) and (23) the amplitude of each output current harmonic is

$$\begin{aligned} C_n &= \sqrt{2}I_{0nr} \\ &= \frac{4\sqrt{2}E}{\pi(n-1)(n+1)n\omega L_f} \\ &= \frac{4}{\pi(n-1)(n+1)n} I_{\text{base}} \end{aligned} \tag{26}$$

which yields the output rms ripple current to be

$$\begin{aligned} I_{0ri} &= \left[\sum_{n=2,4,6,\cdots}^{\infty} I_{0nr}^2\right]^{1/2} \\ &= \left[\sum_{n=2,4,6,\cdots}^{\infty} (C_n/\sqrt{2})^2\right]^{1/2}. \end{aligned} \tag{27}$$

Therefore, the output rms current is

$$I_{0r} = (I_0^2 + I_{0ri}^2)^{1/2} \tag{28}$$

and the input power factor (without $C_i$) in a continuous mode of operation is

$$(\text{PF}) = VI_0/EI_{0r} = VI_0/E(I_0^2 + I_{0ri}^2)^{1/2} \tag{29}$$

or

$$(\text{PF}) = V/E[1 + (I_{0ri}/I_0)^2]^{1/2}. \tag{30}$$

Neglecting all the current harmonics above sixth, the output rms ripple current from (26) and (27) is

$$I_{0ri} = [I_{02r}^2 + I_{04r}^2 + I_{06r}^2]^{1/2} = \left[\sum_{n=2,4,6} \left(\frac{4}{\pi(n-1)(n+1)n\sqrt{2}}\right)^2\right]^{1/2} \cdot I_{base} = 0.1525 I_{base}. \quad (31)$$

Putting (3), (22), and (31) into (30) gives the following expression for the input power factor (without $C_i$) in the continuous mode

$$(PF) = 0.9/[1 + (0.1525/I_{0n})^2]^{1/2} \quad (32)$$

in which $I_{0n} = I_0/I_{base}$ is the normalized average output current.

## DETERMINATION OF THE OPTIMUM OPERATING POINT FOR THE RECTIFIER

The object of this section is to determine the optimum operating point for the bridge rectifier (Fig. 1) from the point of view of maximum input power factor, minimum filter inductance, and minimum output voltage regulation.

For the purpose of relating input power factor and output voltage regulation to filter inductance $L_f$ for various modes of operation, a new parameter "normalized power $P_n$" is defined as follows:

$$P_n = P_0/P_{base} \quad (33)$$

where

$P_0$ = output power

$P_{base}$ = base power = $V_{base} \cdot I_{base}$

$$= 2E^2/\omega L_f. \quad (34)$$

Therefore, if the output power $P_0$ is constant, then the parameter $P_n$ is a measure of filter inductance $L_f$. The parameter $m$ is henceforth used to represent the output dc voltage regulation. The higher the value of $m$, the better the output voltage regulation.

Equation (13) gives the expression for the input power factor for discontinuous modes I and II

$$(PF) = \sqrt{2} m I_{0n}/I_{0rn} = \sqrt{2} m/\text{form factor}. \quad (35)$$

Also, for all modes from (33), (34), and (3), it results in

$$P_n = P_0/P_{base} = VI_0/V_{base} \cdot I_{base} = mI_{0n} \quad (36)$$

where $I_{0n}$ is the normalized average output current. Therefore, for discontinuous modes I and II, (35) and (36) yield

$$(PF) = \sqrt{2} P_n/I_{0rn} \quad (37)$$

while for the continuous mode, (32), (36), and (22) give

$$(PF) = 0.9/[1 + (0.097/P_n)^2]^{1/2}. \quad (38)$$

For all modes, the normalized capacitor voltage from (36) is

$$m = P_n/I_{0n}. \quad (39)$$

### *The Optimum Operating Point*

Fig. 5 shows the variation of the input power factor (without $C_i$) and the normalized capacitor voltage against normalized power for constant output power. The Appendix explains the method used in plotting these curves. In discontinuous mode I the input power factor increases as the normalized capacitor voltage $m$ decreases. Equations (33) and (34) show that the filter inductance requirement for constant output power also increases. However, the power factor curve becomes flat around $m = 0.79$ (PF = 0.763) and then decreases down to a value of 0.731, when the current becomes continuous. In the continuous mode the normalized capacitor voltage remains constant, and increasing filter inductance reduces the ripple current and therefore the power factor increases. In the limit, when filter inductance is infinite, the power factor approaches 0.9.

The reduction in power factor after $m = 0.79$ is due to the changes in the current wave shape in discontinuous mode II. Fig. 6 shows the variation of form factor with normalized capacitor voltage $m$. Below $m = 0.79$, the rate of decrease of the form factor reduces and therefore the power factor reduces.

Fig. 5 shows that if the rectifier output current is discontinuous, the output voltage regulation is low (regulation = $(\sqrt{2}E - V)/V = (1 - m)/m$) and the filter inductance requirement is also low. However, the maximum attainable power factor, with no $C_i$ at the front end of Fig. 1, is only 0.763. If the rectifier output current $i_0$ is continuous, then the power factor is high (around 0.9); however, the output voltage $V$ regulation and the filter inductance requirements are very high.

The optimum operating point in the discontinuous current region is at $m = 0.79$ at which the input power factor is maximum. The output voltage regulation is 27 percent. For the same output power and power factor if the operating point is chosen in the continuous current region, then a filter inductance three times larger is required ($L_{f2}/L_{f1} = P_{n2}/P_{n1} = (1.55 \times 10^{-1})/(5.2 \times 10^{-2}) \simeq 3$) and the normalized capacitor voltage is only $2/\pi$, which yields the voltage $V$ regulation to be 57 percent.

Therefore, from the viewpoint of the power factor, filter inductance requirement, and the output voltage regulation, the overall optimum operating point at rated output power is in the discontinuous current region at which the power factor is maximum.

## SELECTION OF FILTER INDUCTANCE

For the optimum operating point ($m = 0.79$), the value of normalized power $P_n$ from Fig. 5 is given by

$$P_n = 5.2 \times 10^{-2}. \quad (40)$$

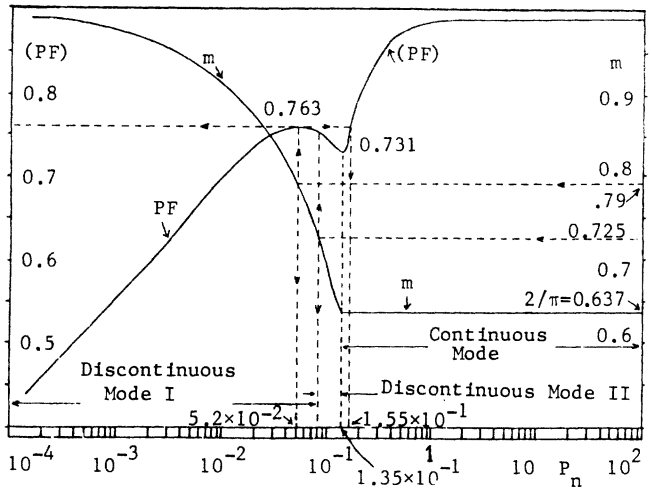


Fig. 5. Variation of input power factor (PF) and normalized capacitor voltage ($m$) versus normalized power ($P_n$) in various modes of rectifier operation for system in Fig. 1.

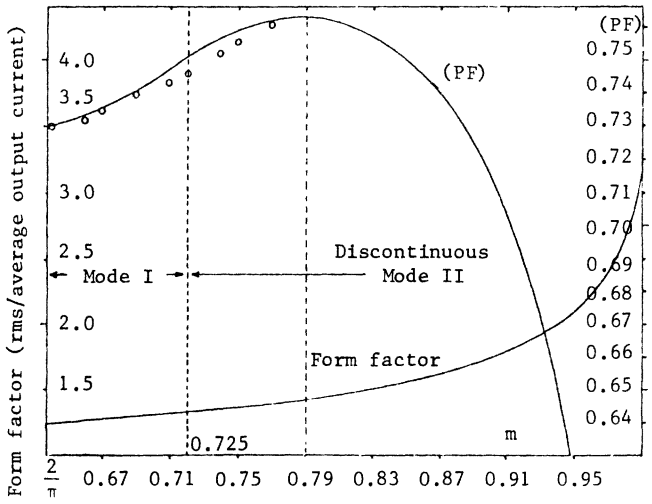


Fig. 6. Variation of input power factor (PF) and form factor versus normalized capacitor voltage ($m$) in discontinuous modes I and II. —— Theoretically predicted. ooo: Experimentally observed.

Therefore, the filter inductance is given by

$$P_n = P_0/P_{\text{base}} = \omega L_f P_0/2E^2$$

or

$$L_f = (2E^2/\omega P_0)P_n \text{ H} \tag{41}$$

where

$\omega$ source frequency in radians per second;
$P_0$ rated output power;
$E$ rms ac voltage.

*Example*

Let $E = 115$ V, $\omega = 377$ rad/s (60 Hz), and $P_0 = 1.2$ kW. Therefore the optimum filter inductance

$$L_f = \frac{2(115)^2 \cdot (5.2 \times 10^{-2})}{377 \times 1200}$$

$$= 3 \text{ mH}.$$

## INPUT POWER FACTOR IMPROVEMENT

For any power supply, an input power factor of at least 0.8 is desirable. However, for the optimum operating point chosen in the preceeding section, the input power factor is only 0.763 and therefore needs further improvement. Power factor improvement by means of a front end capacitor $C_i$ (Fig. 1) is discussed in this section. The value of $C_i$ is selected such that the fundamental input power factor at rated load is unity. The normalized rectifier input current $i_{an}$ for discontinuous mode I (Fig. 1) is represented by the following Fourier series:

$$i_{an} = \sum_{n=1}^{\infty} G_n \cos n\omega t + \sum_{n=1}^{\infty} H_n \sin n\omega t \tag{42}$$

$$G_n = \frac{1}{\pi}\int_0^{2\pi} i_{an} \cos n\omega t \, d\omega t$$

$$= \frac{2}{\pi}\left[\int_{\alpha}^{\alpha+\gamma} i_{0n} \cos n\omega t \, d\omega t\right], \qquad n \text{ odd} \tag{43}$$

$$H_n = \frac{2}{\pi}\left[\int_{\alpha}^{\alpha+\gamma} i_{0n} \sin n\omega t \, d\omega t\right], \qquad n \text{ odd} \tag{44}$$

where $i_{0n}$ is given by (10). Therefore

$$i_{an} = \sum_{n \text{ odd}} K_n \sin(n\omega t + \theta_n) \tag{45}$$

where the source voltage $v_s = \sqrt{2}E \sin \omega t$ is the reference and

$$K_n = (G_n^2 + H_n^2)^{1/2} \tag{46}$$

$$\theta_n = \tan^{-1}(G_n/H_n). \tag{47}$$

For the optimum operating point ($m = 0.79$), the values of $K_n$ and $\theta_n$ are summarized in Table I. The value of $C_i$ to improve the fundamental power factor to unity is derived from Fig. 7, in which $I_{C_i}$, $I_{a1r}$ and $I_{i1r}$ are the rms values of the fundamental components of capacitor $C_i$, rectifier input, and total input currents, respectively. Therefore,

$$\frac{E}{X_{C_i}} = \frac{\sqrt{2}E}{\omega L_f} \cdot \frac{0.121 \sin 30.97^\circ}{\sqrt{2}}$$

or

$$\omega C_i = 0.121 \sin 30.97^\circ/\omega L_f. \tag{48}$$

The apparent input power factor after installation of capacitor $C_i$ is

$$\text{PF}^* = V \cdot I_{0n}/(EI_{irn}) = \sqrt{2}m \cdot I_{0n}/I_{irn} \tag{49}$$

in which $I_{0n}$ and $I_{irn}$ are the normalized, average output current ($m = 0.79$), and rms input current, respectively.

$$I_{0n} = 0.066, \qquad \text{for } m = 0.79$$

$$I_{irn} = \frac{1}{\sqrt{2}}[I_{i1r}^2 + I_{i3r}^2 + I_{i5r}^2]^{1/2}$$

$$= \frac{1}{\sqrt{2}}[I_{i1r}^2 + I_{a3r}^2 + I_{a5r}^2]^{1/2} \tag{50}$$

TABLE I
FOURIER COEFFICIENTS OF THE INPUT CURRENT WAVEFORM FOR THE OPTIMUM OPERATING POINT OF THE RECTIFIER ($m = 0.79$)

| Harmonic Number | $K_n$ | $\theta_n$ (deg) |
|---|---|---|
| 1 | 0.121 | −30.97 |
| 3 | 0.060 | 81.41 |
| 5 | 0.012 | −41.66 |
| 7 | 0.009 | −13.29 |
| 9 | 0.005 | 5.77 |
| 11 | 0.003 | 44.04 |
| 13 | 0.002 | 63.88 |
| 15 | 0.001 | 88.74 |

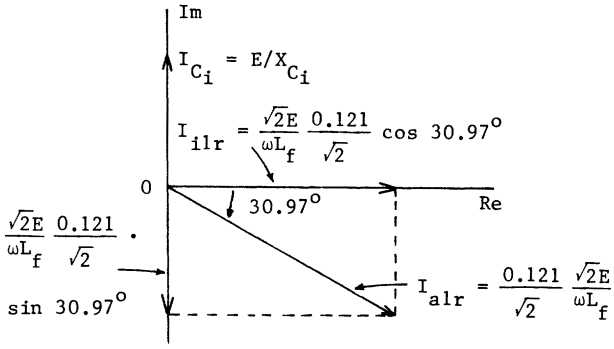


Fig. 7. Phasor diagram of currents for improvement of fundamental input power factor by front end capacitor $C_i$.

or

$$I_{irn} = \frac{1}{\sqrt{2}} [(0.21 \cos 30.97^\circ) + 0.06^2 + 0.012^2]^{1/2}$$

$$= 0.0852$$

$$PF^* = \sqrt{2} \times 0.79 \times 0.066/0.0852 = 0.865. \quad (51)$$

## SELECTION OF FILTER CAPACITANCE $C_f$

The detailed analysis regarding the selection of filter capacitance $C_f$ is given in [4]. This analysis is basically based on the calculation of the rms ripple voltage across $C_f$ in mode I (the optimum operating point lies in this mode), neglecting the high frequency ripple due to the dc-to-dc converter or inverter connected to $C_f$ and considering only the 120-Hz ripple from the rectifier output. The value of $C_f$ for 5 percent harmonics on the capacitor voltage at the optimum operating point ($m = 0.79$) from [4] is given by

$$C_f = 10P_n/m^2\omega^2 L_f. \quad (52)$$

*Example*

For the optimum operating point $P_n = 5.2 \times 10^{-2}$, $m = 0.79$, $\omega = 377$ rad/s (60 Hz) and $L_f = 3$ mH. Therefore,

$$C_f = 10 \times (5.2 \times 10^{-2})/(0.79)^2(377)^2(3 \times 10^{-3})$$

$$= 1954 \times 10^{-6} \text{ F}$$

$$= 1954\ \mu\text{F}.$$

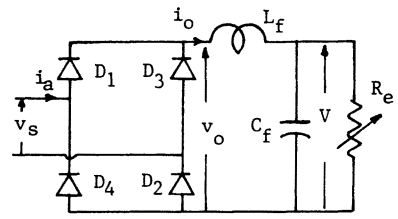


Fig. 8. Circuit used in obtaining experimental results.

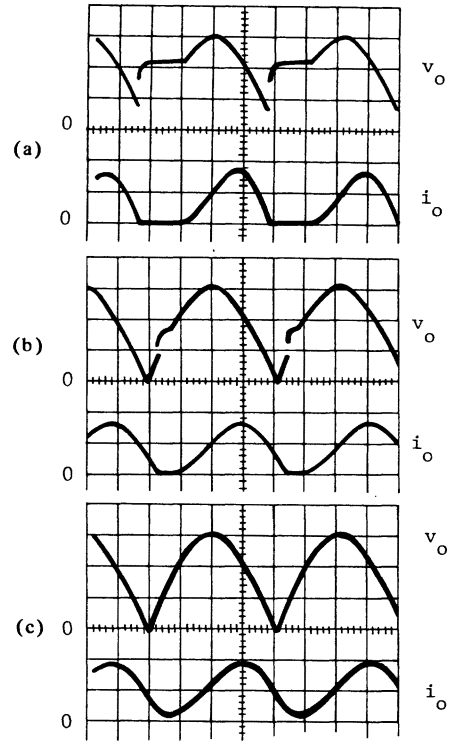


Fig. 9. Oscillograms of rectifier output voltage $v_0$ and output current $i_0$ in different modes of operaion of system shown in Fig. 8. Upper trace 50 V/div, 2 ms/div. Lower trace 10 A/div, 2 ms/div. (a) Discontinuous mode I. (b) Discontinuous mode II. (c) Continuous mode.

## EXPERIMENTAL VERIFICATION

Fig. 8 shows the circuit used in obtaining the experimental values of the form factor specified in Fig. 6. Also, the experimental waveforms of the rectifier output voltage $v_0$ and output current $i_0$ in different modes of operation are shown in Fig. 9.

## CONCLUSION

Theoretical results presented in this paper have been verified experimentally and the agreement is close [4]. This paper has shown that the input power factor does not monotonically increase with increasing filter inductance. Consequently, the optimum rectifier operating point has been shown to lie in the discontinuous mode. Significant power factor improvement can be achieved by installing a front end capacitance. A design procedure has been described and illustrated by a numerical example.

## APPENDIX

The curves in Fig. 5 apply to the operation of the rectifier of Fig. 1 in discontinuous modes I, II, and the continuous

mode. The value of $m$ establishes the criterion for distinction of these three modes. In the continuous mode, $m$ is constant and equal to $2/\pi$. To find the value of $m$ bordering discontinuous modes I and II, (4) and (7) are solved such that $\alpha + \gamma = \pi$. In this case it results in

$$\gamma = 133.5^\circ \qquad \alpha = 46.5^\circ \qquad m = 0.725.$$

To plot $m$ and (PF) versus $P_n$ for mode I, the value of $m$ is changed such that $1 > m \geqslant .725$ (for $m = 1$, $\alpha = 90^\circ$ and $\gamma = 0^\circ$). For each value of $m$, $\alpha$ is calculated from (4), $\gamma$ from (7), $I_{0n}$ from (11), $I_{0rn}$ from (12), $P_n$ from (36), and (PF) from (37). In mode II, $m$ is changed such that $0.725 > m \geqslant 2/\pi$. For each value of $m$, $\alpha$ is obtained from (4), $I_{0\pi n}$ from (14), $\omega t_1'$ from (17), $\gamma$ from (18), $I_{0n}$ from (19), $I_{0rn}$ from (20), $P_n$ from (36), and (PF) from (37). For the continuous mode, $m$ remains constant and equal to $2/\pi$. The value of (PF) is calculated from (33) in which $P_n$ is varied from the last value obtained for mode II with $m = 2/\pi$ ($P_n \simeq 1.35 \times 10^{-1}$), up to such a value beyond which no substantial increase in power factor is noticed ($P_n \simeq 10^2$).

## REFERENCES

[1] S. B. Dewan and A. Straughen, *Power Semiconductor Circuits*. New York: Wiley, 1975, pp. 426–444.

[2] B. D. Bedford and R. Hoft, *Principles of Inverter Circuits*. New York: Wiley, 1964, pp. 128–141.

[3] S. Lindena, "PWM series inverter with inductor-transformer in low power applications," in *Conf. Rec. IEEE Power Conditioning Specialists*, 1971.

[4] P. Shively, "Analysis and design of an output clamped inverter," M.A.Sc. thesis, University of Toronto, Toronto, ON, Canada, Department of Electrical Engineering, 1978.

**Shashi B. Dewan** (S'65–M'67–SM'68), for a photograph and biography, please see page 40 of the January/February issue of this TRANSACTIONS.